



# Fusion of $^{40}\text{Ca} + ^{96}\text{Zr}$ revisited: Transfer couplings and hindrance far below the barrier



A.M. Stefanini<sup>a,\*</sup>, G. Montagnoli<sup>b</sup>, H. Esbensen<sup>c</sup>, L. Corradi<sup>a</sup>, S. Courtin<sup>d</sup>, E. Fioretto<sup>b</sup>,  
A. Goasduff<sup>e</sup>, J. Grebosz<sup>f</sup>, F. Haas<sup>d</sup>, M. Mazzocco<sup>b</sup>, C. Michelagnoli<sup>b</sup>, T. Mijatović<sup>g</sup>,  
D. Montanari<sup>b</sup>, G. Pasqualato<sup>b</sup>, C. Parascandolo<sup>b</sup>, F. Scarlassara<sup>b</sup>, E. Strano<sup>b</sup>, S. Szilner<sup>g</sup>,  
D. Torresi<sup>b</sup>

<sup>a</sup> INFN, Laboratori Nazionali di Legnaro, I-35020 Legnaro (Padova), Italy

<sup>b</sup> Dipartimento di Fisica e Astronomia, Università di Padova, and INFN, Sez. di Padova, I-35131 Padova, Italy

<sup>c</sup> Physics Division, Argonne National Laboratory, Argonne, IL 60439, USA

<sup>d</sup> IPHC, CNRS-IN2P3, Université de Strasbourg, F-67037 Strasbourg Cedex 2, France

<sup>e</sup> CSNSM, CNRS/IN2P3 and Université Paris-Sud, F-91405 Orsay Campus, France

<sup>f</sup> Institute of Nuclear Physics, Polish Academy of Sciences, PL 31-342 Cracow, Poland

<sup>g</sup> Ruđer Bošković Institute, HR-10002 Zagreb, Croatia

## ARTICLE INFO

### Article history:

Received 25 October 2013

Received in revised form 19 December 2013

Accepted 19 December 2013

Available online 27 December 2013

Editor: V. Metag

### Keywords:

Heavy-ion fusion

Sub-barrier cross sections

Coupled-channels model

## ABSTRACT

The sub-barrier fusion excitation function of  $^{40}\text{Ca} + ^{96}\text{Zr}$  has been measured down to cross sections  $\simeq 2.4 \mu\text{b}$ , i.e. two orders of magnitude smaller than obtained in a previous experiment, where the sub-barrier fusion of this system was found to be greatly enhanced with respect to  $^{40}\text{Ca} + ^{90}\text{Zr}$ , and the need of coupling to transfer channels was suggested relying on coupled-channels calculations. The purpose of this work has been to investigate the behavior of  $^{40}\text{Ca} + ^{96}\text{Zr}$  fusion far below the barrier, thereby disentangling the elusive interplay of effects due to inelastic couplings, transfer couplings and, possibly, the appearance of the fusion hindrance. The smooth trend of the excitation function has been found to continue, and the logarithmic slope increases very slowly. No indication of hindrance shows up, and a comparison with  $^{48}\text{Ca} + ^{96}\text{Zr}$  is illuminating in this respect. A new CC analysis of the complete excitation function has been performed, including explicitly one- and two-nucleon  $Q > 0$  transfer channels. Such transfer couplings bring significant cross section enhancements, even at the level of a few  $\mu\text{b}$ . Locating the hindrance threshold, if any, in  $^{40}\text{Ca} + ^{96}\text{Zr}$  would require challenging measurements of cross sections in the sub- $\mu\text{b}$  range.

© 2013 The Authors. Published by Elsevier B.V. Open access under CC BY license.

## 1. Introduction

Heavy-ion fusion reactions at sub-barrier energies display a wide range of attractive features that have been the object of a multitude of investigations. The starting point was the discovery of strong and systematic cross section enhancements near and below the barrier, that have been associated to couplings of the relative motion to nuclear shape deformations and vibrations [1]. The more recent discovery [2] of the hindrance phenomenon at very low

energies, has made the situation even more appealing, but more complex as well.

On the other hand, the role of couplings to nucleon transfer channels has never been unambiguously identified, after the innovating experiments of Beckerman et al. [3] on the various Ni + Ni systems, and the early suggestion of Broglia et al. [4] that two-neutron transfer with  $Q > 0$  should enhance sub-barrier fusion. Nucleon transfer effects should show up rather clearly down to energies well below the barrier, just where hindrance is expected, thus fusion cross sections are determined by the concurring contributions of hindrance and enhancement in that energy range. The requirement to place on more solid bases, theoretical predictions where very neutron-rich exotic beams are used, is generally felt. Indeed, in those cases large effects on sub-barrier fusion cross sections are qualitatively expected, but not systematically found [5,6].

The fusion of  $^{40}\text{Ca} + ^{96}\text{Zr}$  was investigated in [7] and its cross section was found to be greatly enhanced with respect to

\* Corresponding author.

E-mail address: alberto.stefanini@lnl.infn.it (A.M. Stefanini).

$^{40}\text{Ca} + ^{90}\text{Zr}$ . Its excitation function decreases remarkably slowly below the barrier, and the barrier distribution has a long tail toward low energies. CC calculations including low-lying surface vibrations, while nicely fitting the  $^{40}\text{Ca} + ^{90}\text{Zr}$  excitation function, strongly underestimated the sub-barrier cross sections of  $^{40}\text{Ca} + ^{96}\text{Zr}$ . Neutron transfer channels with positive  $Q$ -values, only existing in  $^{40}\text{Ca} + ^{96}\text{Zr}$ , were suggested to be the reason of the difference.

The concept of fusion barrier distribution is inherent in the coupled-channels model, where positive  $Q$ -value neutron transfer reactions give rise to barrier(s) lower in energy than the uncoupled one. This is the basic underlying reason why such transfer couplings should enhance fusion cross sections at low energies (see [8] and references therein).

The  $^{40}\text{Ca} + ^{90,96}\text{Zr}$  excitation functions were correctly fit by Zagrebaev [9] using a simplified model for neutron transfer, as well as by the quantum molecular dynamics model of Wang et al. [10,11], but it was also proposed [12,13] that the difference between the two systems is mainly due to the strong octupole vibration of  $^{96}\text{Zr}$ . This disagrees with the results of the subsequent experiment on  $^{40}\text{Ca} + ^{94}\text{Zr}$  [14] indicating that this system (having  $Q > 0$  neutron transfer channels) behaves exactly as  $^{40}\text{Ca} + ^{96}\text{Zr}$ , in spite of the weak octupole excitation of  $^{94}\text{Zr}$  (comparable to that of  $^{90}\text{Zr}$ ). The full comparison of the four systems  $^{40,48}\text{Ca} + ^{90,96}\text{Zr}$  [15,16] suggested that neutron transfer does play a role in  $^{40}\text{Ca} + ^{96}\text{Zr}$ .

The recent theoretical work of V.V. Sargsyan et al. (see [17] and references therein) presents sub-barrier cross sections for  $^{40}\text{Ca} + ^{96}\text{Zr}$  down to values of 3  $\mu\text{b}$ . The use of a double folding potential, and the influence of fluctuations and dissipation in the quantum-diffusion approach to barrier penetration, results in a remarkably good fit to the sub-barrier data of the previous experiment [7]. In a subsequent article [18], those authors encouraged further experimental measurements of very small fusion cross sections in this (and other) systems, and, very recently, the role of neutron-pair transfer reactions in sub-barrier capture processes was emphasized [19].

In lighter cases, analogous systematic trends have been observed. The effect of transfer is strong and clear in  $^{40}\text{Ca} + ^{48}\text{Ca}$  [20,21], whose cross sections exceed the  $^{48}\text{Ca} + ^{48}\text{Ca}$  data at low energies and are suppressed compared to the  $^{40}\text{Ca} + ^{40}\text{Ca}$  data at high energies. The same enhancement/suppression effect is observed for  $^{32}\text{S} + ^{48}\text{Ca}$  with respect to  $^{36}\text{S} + ^{48}\text{Ca}$  [22]. It is possible to account for the fusion cross sections of  $^{40}\text{Ca} + ^{48}\text{Ca}$  and  $^{32}\text{S} + ^{48}\text{Ca}$  by including couplings to one- and two-nucleon transfer channels with positive  $Q$ -values and by adjusting the strength and the effective  $Q$ -value of the pair transfer. Further recent examples of effects due to transfer couplings are reported in Refs. [23,24].

The situation is different when considering heavier and soft systems. The investigation of  $^{60,64}\text{Ni} + ^{100}\text{Mo}$  [25] brings evidence of the two excitation functions being very similar to each other down to  $\simeq 2 \mu\text{b}$ . Transfer couplings to  $Q > 0$  channels in  $^{60}\text{Ni} + ^{100}\text{Mo}$  appear to play a marginal role, and hindrance appears for the system with  $^{64}\text{Ni}$  in the sub- $\mu\text{b}$  range. Analogously, systematic studies of several combinations of nickel and tin isotopes evidenced very similar sub-barrier excitation functions [26], in spite of the strongly varying  $Q$ -values for few-neutron transfer channels. Detailed calculations for  $^{58}\text{Ni} + ^{124}\text{Sn}$  [27] for which complete sets of data exist for fusion, elastic and inelastic scattering, and few- and multi-nucleon transfer channels [28], indicate that couplings to the neutron transfer channels do enhance the sub-barrier fusion cross sections, but the enhancement is much weaker than the effect of dominating couplings to the strong low-lying surface modes.

The Ca + Zr systems are intermediate cases. For  $^{40}\text{Ca} + ^{96}\text{Zr}$ , in particular, the lowest fusion cross section previously reported [7] is  $\sigma = 0.16 \text{ mb}$ . However, this corresponds to an energy which is too large 1) to reveal the possible appearance of fusion hindrance, and 2) to try disentangling the elusive interplay of effects due to inelastic couplings, transfer couplings and fusion hindrance, with the help of coupled-channels (CC) calculations. These two points were the purpose of the experiments reported here, that have used our upgraded set-up allowing the measurement of very small cross sections.

The present new results have extended the excitation function by almost two orders of magnitude down to  $\sigma \simeq 2.4 \mu\text{b}$ . CC calculations in the spirit of those of Ref. [7] have also been performed. However, in the present case couplings to one- and two-nucleon transfer channels have explicitly been included, using the same formalism employed for the analysis of heavier ( $^{58}\text{Ni} + ^{124}\text{Sn}$  [27]) and lighter ( $^{32}\text{S} + ^{48}\text{Ca}$  [22]) systems.

## 2. Experimental set-up and results

Fusion-evaporation cross sections have been measured for  $^{40}\text{Ca} + ^{96}\text{Zr}$  at several energies from well below to well above the nominal Coulomb barrier  $V_b \simeq 139 \text{ MeV}$ , using the  $^{40}\text{Ca}$  beams of the XTU Tandem accelerator of INFN – Laboratori Nazionali di Legnaro (LNL). The five lowest measured energies (120, 121, 122, 123, 124 MeV) are below the limit of the previous experiment [7], while the three highest ones (140, 146, 152 MeV) have been used to fix the absolute cross section scale using the earlier data as a reference. Additional intermediate energies (125.5, 128, 134 MeV) have been measured as well.

The beam energy of the Tandem XTU accelerator of LNL is determined to better than 1/800 in an absolute scale [29], that is, 150 keV at  $E_{\text{lab}} = 120 \text{ MeV}$ . The energy was varied only downwards starting from 152 MeV, and for each energy the beam was focused to the same position in the target plane using a fluorescent quartz.

The beam intensity was  $\simeq 5 \text{ pA}$  (up to 10 pA in some cases), and the targets were 50  $\mu\text{g}/\text{cm}^2$  evaporations of isotopically enriched zirconium on carbon backings 15  $\mu\text{g}/\text{cm}^2$ , containing 1.16%  $^{90}\text{Zr}$ , 0.30%  $^{91}\text{Zr}$ , 0.55%  $^{92}\text{Zr}$ , 1.28%  $^{94}\text{Zr}$ , and 96.71%  $^{96}\text{Zr}$ . This isotopic composition was taken into account in the data analysis, using also the measured excitation functions of  $^{40}\text{Ca} + ^{90,94}\text{Zr}$  [7,14].

$^{96}\text{Zr}$  is the heaviest stable zirconium isotope, hence the other isotopes produce higher Coulomb barriers in the laboratory system. For example,  $^{40}\text{Ca} + ^{90,94}\text{Zr}$  have barriers  $\simeq 1.5 \text{ MeV}$  and 4.5 MeV higher. This leads to negligible corrections to the cross sections, particularly at low energies. Possible (unobserved) contaminations from elements with  $Z < 40$  in the target would have produced ER much lighter than  $^{96}\text{Zr}$  (at least 8–10 mass units apart), easily separated out by means of our combined Energy–Time-of-Flight (TOF) measurements.

Evaporation residues (ER) were detected at  $0^\circ$  and at small angles by a  $\Delta E$ – $E$ –TOF telescope following beam rejection with the electrostatic deflector (see Refs. [22,29] for details) systematically used for sub-barrier fusion measurements at LNL. Fusion–fission is negligible for  $^{40}\text{Ca} + ^{96}\text{Zr}$  in the considered energy range, so fusion-evaporation cross sections have been identified with total fusion cross sections.

Fig. 1 shows two examples of Energy–TOF two-dimensional spectra taken during the measurements. At the lower (higher) beam energy 123 (134) MeV, the spectrum was taken in a run of  $\simeq 6$  (3) hours with a beam intensity of  $\approx 8$  (4) pA, and 11 ( $\simeq 1200$ ) ER were detected. The excitation function is shown in Fig. 2. The smallest cross section  $\simeq 2.4 \mu\text{b}$  was measured at  $E_{\text{lab}} = 120 \text{ MeV}$ , that is, about 14% below the nominal Coulomb barrier.

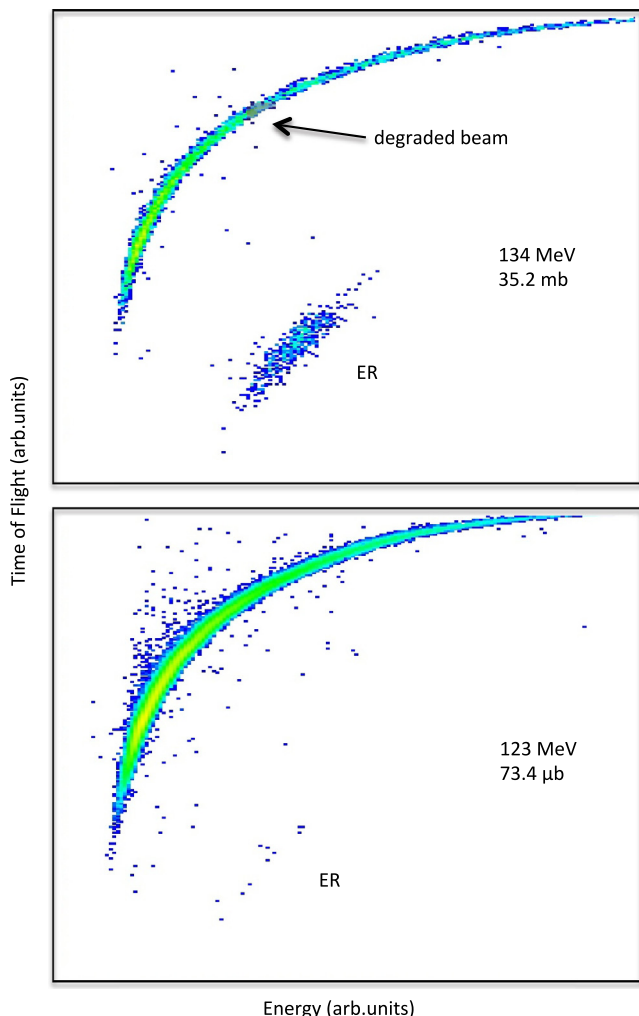


**Fig. 1.** (Color online.) Two-dimensional Energy–TOF spectra obtained in the present experiment around (top) and below (bottom) the barrier.

### 3. Coupled-channels analysis

A new CC analysis has been performed, using a Woods–Saxon (WS) ion–ion potential. A different prescription (like, e.g., a M3Y + repulsion potential [31,32]) is not required, because we have no indication of hindrance in this system, as we shall see in the following. The calculations are based on the WS potential derived from the Akyüz–Winther (AW) expression [33] with parameters  $V_0 = -73.98$  MeV,  $R = 9.599$  fm ( $r_0 = 1.18$  fm) and  $a = 0.673$  fm, and the CC equations are solved using the same formalism described, e.g., in Refs. [22,30]. The potential has been slightly modified so that the full calculation (Ch-69, see below) reproduces the data above 100 MeV, where the best normalized  $\chi^2/N = 1.8$  is achieved with a radius shift  $\Delta R = 0.18$  fm. This produces a barrier  $V_b = 96.62$  MeV.

The results of the calculations are certainly sensitive to the potential parameters, in particular to its diffuseness. Indeed, in various recent studies (see e.g. Refs. [34,35]) the appearance of low-energy hindrance has been “simulated” by using WS potentials with anomalously large diffuseness. This is why M3Y + repulsion double-folding potentials (shallow potentials [31,32]) have been introduced. In the present case of  $^{40}\text{Ca} + ^{96}\text{Zr}$  no hindrance is observed, and cross sections are underestimated when using a standard diffuseness, as we shall see here below. This means that

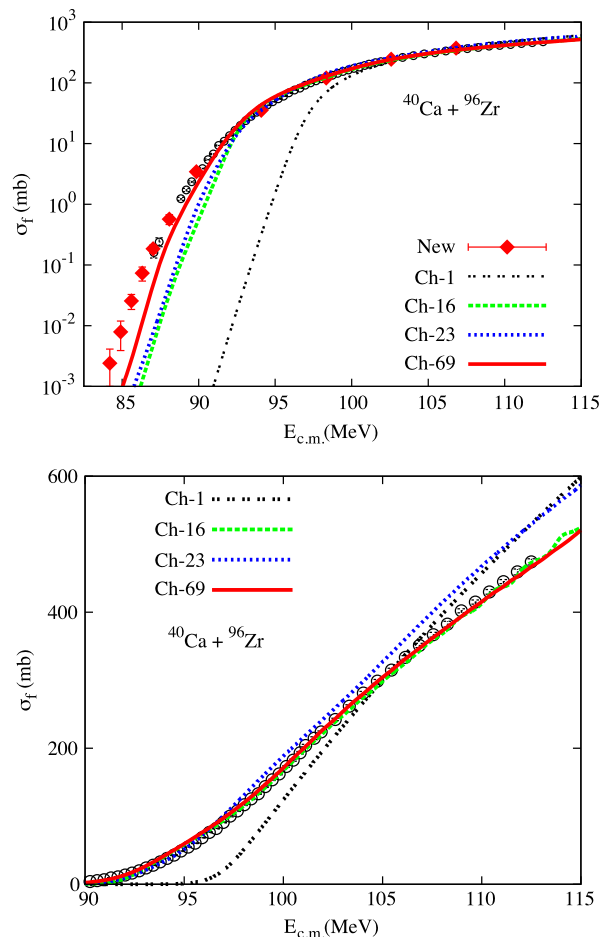


**Fig. 2.** (Color online.) Excitation function of  $^{40}\text{Ca} + ^{96}\text{Zr}$  in a logarithmic (top) and linear (bottom) scale. The red and black symbols are the cross sections measured in this work and in Ref. [7], respectively. Here and in the following figures, only statistical uncertainties are reported. The lines are the results of the CC calculations described in the text (Ch-1 is the no-coupling limit).

**Table 1**

Adopted structure of the excited states in  $^{40}\text{Ca}$  and the Zr isotopes. The input for  $^{40}\text{Ca}$  is from Ref. [36]. The input for  $^{96}\text{Zr}$  is from [37], except the octupole which is from [38].

	$\lambda^\pi$	$E_x$ (MeV)	$B(E\lambda)$ ( $e^2b^{2\lambda}$ )	$\beta_\lambda^C$	$\sigma_\lambda^C$ (fm)	$\sigma_\lambda^N$ (fm)
$^{40}\text{Ca}$	$2^+$	3.904	2.26(14)	0.119	0.138	0.125
	$3^-$	3.737	27(4)	0.402	0.465	0.315
	$5^-$	4.491		0.297	0.344	0.175
$^{96}\text{Zr}$	$2^+$	1.751	4(3)	0.079	0.123	0.123
	$3^-$	1.897	53(6)	0.285	0.441	0.441

an even smaller diffuseness (producing a narrow barrier) would be required to fit the sub-barrier data, which is rather unrealistic.

The nuclear structure information used for the calculations is reported in Table 1. For  $^{40}\text{Ca}$ , the level energies and spectroscopic properties of Ref. [36] were adopted. The calculations also include the two-phonon excitations of the  $2^+$  and  $3^-$  states and mutual excitations of projectile and target. That gives a total of 16 channels and the calculation is called Ch-16. The results are sensitive to multi-phonon excitations because of the strong octupole excitation in  $^{96}\text{Zr}$ . Similar to the recent analysis of the  $^{48}\text{Ca} + ^{96}\text{Zr}$  fusion data [42] we therefore include up to three-phonon excitations of this mode assuming that it is harmonic. We exclude mutual excitations in the same nucleus in order to limit the number of channels.

This results in 23 channels (Ch-23), instead of the 16 channels in the Ch-16 calculation mentioned above.

The calculations Ch-23 and Ch-16 do not differ too much from each other, and both of them strongly underestimate the sub-barrier cross sections. There is a clear need for additional (transfer) couplings at energies below 95 MeV, as pointed out in Ref. [7]. This is confirmed, and made even more clear, by the new low-energy measurements presented in this article. Therefore, we consider explicitly in the CC calculations the influence of transfer on the fusion of  $^{40}\text{Ca} + ^{96}\text{Zr}$ .

The ground state  $Q$ -values for one- and two-neutron pick-up channels are all positive ( $Q_{1n} = 0.51$  MeV,  $Q_{2n} = 5.5$  MeV). We include one-nucleon transfer couplings following the conventional shell-model description of the relevant nuclear states [39], used e.g. in Ref. [27] and more recently in [22]. Two-nucleon transfer channels were simulated in the calculations by one pair-transfer channel with an effective  $Q$ -value = 1 MeV and using the macroscopic form factor proposed by Dasso and Vitturi [40], with a transfer strength  $\sigma_{2n} = 0.5$  fm. The calculation has a total of 69 channels (Ch-69) and gives the best fit to the data above 90 MeV, see Fig. 2 (bottom), with a  $\chi^2/N = 2$ . The large 2n-strength may reflect that two-proton transfer also has a positive  $Q$ -value and gives a contribution. As recently calculated for  $^{32}\text{S} + ^{48}\text{Ca}$  [22], the largest effect on sub-barrier fusion is originated by the pair transfer 2N (2n and 2p). The contribution of the one-nucleon transfer is calculated to be quite negligible, and it is not shown separately in Fig. 2 for clarity.

In any case, it is seen that the full calculation Ch-69 underestimates the measured excitation function at the lowest energies, even if the pair transfer is included in the coupling scheme in an approximate and schematic way.

A hint on how one could improve the CC results comes from looking at the situation above the barrier. This is done in the linear plot of the excitation function of Fig. 2 (bottom), where the Ch-16 calculation fits the data, the Ch-23 calculation exceeds them at high energies, but the influence of transfer in the Ch-69 calculation restores the agreement. Increasing the 2N transfer strength would reduce the calculated cross section at high energy, while increasing the number of multi-phonon states would enhance that cross section. Hence, one way to improve the calculations below the barrier would be to include more multi-phonon excitations and increase the strength of the pair transfer. Another way is to include nuclear couplings of higher order in the surface distortion (the model used here goes only to the 2nd order [41]).

The present calculations are based on the premise that excitations and transfer are independent processes. Therefore, the ion potentials are taken to be the same for the initial and final mass partition of the fusing system. Of course, this may be inadequate to describe the dynamic evolution of the system toward fusion, since it is not a valid assumption if the deformation is different for the final mass partition.

In analogy with the two panels of Fig. 2, Fig. 3 shows the logarithmic (top) and linear (bottom) derivative of the energy-weighted excitation function,  $L(E)$  and  $d(E\sigma)/dE$  respectively. As remarked above, the experimental slope  $L(E)$  remains small, and increases smoothly down to the lowest measured energies. The calculation Ch-69 is not far from the data. The trend suggested by the previous data at higher energies is confirmed by the present measurements, in agreement also with the phenomenological analysis of Ref. [42]. Locating the hindrance threshold in  $^{40}\text{Ca} + ^{96}\text{Zr}$  is therefore a serious experimental challenge that will require cross section measurements in the sub- $\mu\text{b}$  range.

The first derivative of the energy-weighted cross section, as calculated in Ch-69, is in remarkably good agreement with the data, in particular at high energies (bottom panel). We show in Fig. 4 the

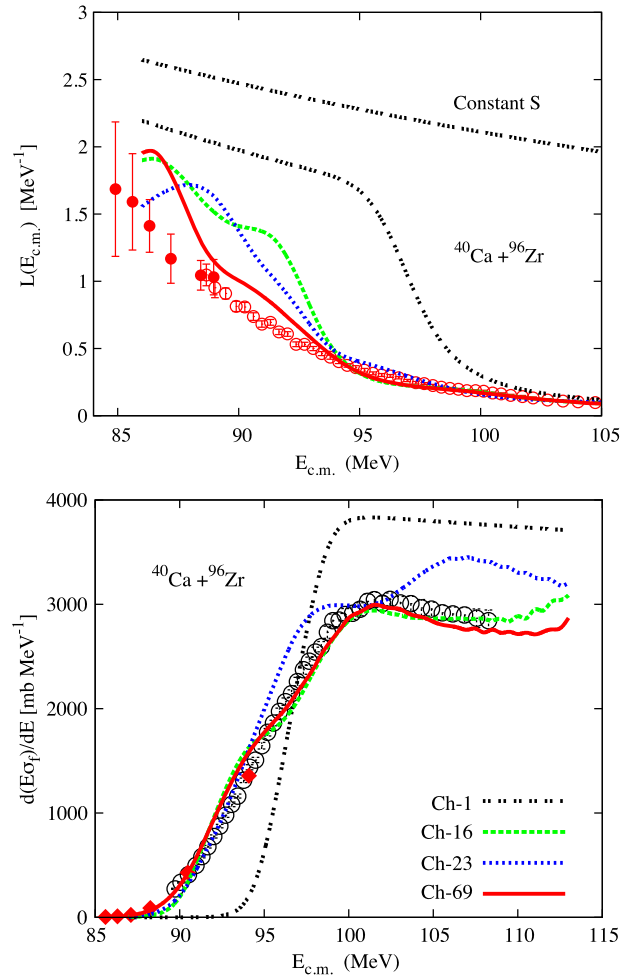


Fig. 3. (Color online.) (Top) Logarithmic derivative (slope) of the fusion excitation function, obtained using both present and previous data, compared to CC results. The slope expected for a constant S factor ( $L_{CS}$ ) is also reported. (Bottom) First derivative of the energy-weighted cross section.

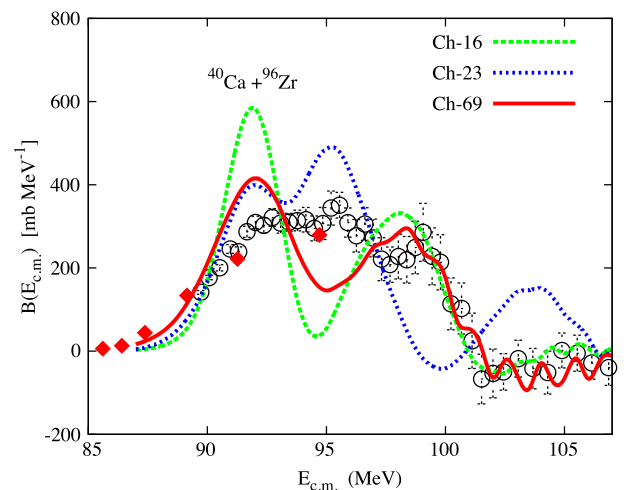
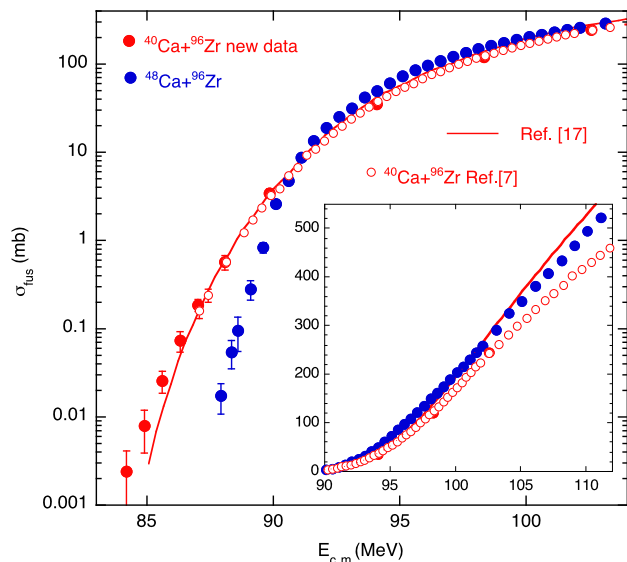


Fig. 4. (Color online.) Barrier distribution of  $^{40}\text{Ca} + ^{96}\text{Zr}$ , compared to CC calculations (see text).

fusion barrier distribution (BD) extracted from the excitation function. We point out that its low-energy side has been completed by the new set of data (full red dots), which clearly show that the BD smoothly vanishes around 87 MeV. In the comparison with the



**Fig. 5.** (Color online.) Fusion cross sections of  $^{40,48}\text{Ca} + ^{96}\text{Zr}$ . The inset shows the two excitation functions in a linear scale. The line is the calculation of Ref. [17] for  $^{40}\text{Ca} + ^{96}\text{Zr}$  (see text).

CC calculations shown in the figure, the unusual width and overall shape of the BD are best reproduced by the Ch-69 calculation including transfer.

As the last point of this section, we compare the extended excitation function including the present new data with the result of the alternative approach of Sargsyan et al. [17]. This is done in Fig. 5, where the red line reports the calculation of that work. The previous data [7] are nicely reproduced, however, the new low-energy data tend to be underestimated, even if the calculation is nearer to the experiment than the prediction of the CC model presented here above. On the other hand, the linear plot (in the inset of Fig. 5) shows that the cross sections above the barrier are overestimated by up to 20% in Ref. [17].

#### 4. Fusion hindrance

There is no indication for the fusion hindrance effect in  $^{40}\text{Ca} + ^{96}\text{Zr}$ . Indeed, the logarithmic slope is very small compared to  $L_{CS}$  even well below the barrier, and the excitation function is even underestimated when using a standard WS potential in the CC calculations. Whether this situation is “simply” due to the strong transfer couplings that push the hindrance threshold lower in energy than the measured range, or it is the consequence of a different mechanism for deep sub-barrier in this system, cannot be inferred by the available data and calculations. Similarly, some systems with positive  $Q$ -values for transfer channels do not show evidence of hindrance, among them,  $^{58}\text{Ni} + ^{64}\text{Ni}$  [3] and  $^{32}\text{S} + ^{48}\text{Ca}$  [22]. However, this does not hold for other cases, e.g.  $^{40}\text{Ca} + ^{48}\text{Ca}$  [20,21] and  $^{28}\text{Si} + ^{64}\text{Ni}$  [43], where hindrance has been recognized clearly.

The present new data allow performing a significant comparison with the low-energy behavior of the excitation function of  $^{48}\text{Ca} + ^{96}\text{Zr}$ . This is done in Fig. 5: the cross section for  $^{48}\text{Ca} + ^{96}\text{Zr}$  decreases very sharply below the barrier and, indeed, this system shows hindrance (see also Refs. [14,42]). On the contrary, the decrease of the excitation function for  $^{40}\text{Ca} + ^{96}\text{Zr}$  is by far slower. The inset is the same plot with a linear cross section scale, where the focus is on the energy range above the barrier. Beyond the trivial Coulomb barrier difference between the two systems, the slope is obviously smaller for  $^{40}\text{Ca} + ^{96}\text{Zr}$ . In the CC model, see above, this is explained by the strong transfer couplings in this system.

#### 5. Summary

In conclusion, we have measured very small fusion cross sections for the system  $^{40}\text{Ca} + ^{96}\text{Zr}$ , whose excitation function has been extended by around two orders of magnitude below the previous limit. The present new measurements reveal a regular trend of the cross sections down to  $\simeq 2.4 \mu\text{b}$ , as well as a logarithmic slope increasing slowly and remaining very low with respect to the constant  $S$  factor value that would be reached, phenomenologically speaking, when a hindrance develops.

The present new data, and the excitation function of Ref. [7] have been analyzed by CC calculations using Woods–Saxon potentials. The nuclear structure of the two colliding nuclei has been taken into account by including the  $2^+$  states and multi-phonon excitations of the collective  $3^-$  excitations. The excitation function is strongly underestimated below a few mb, and there is a clear need for additional couplings. One- and two-nucleon transfer channels have been explicitly included in the calculations, where the largest effect on sub-barrier fusion comes from the pair transfer. This makes the data fit much better, however, the sub-barrier data are still underpredicted. A further comparison with the results of the quantum-diffusion approach to barrier penetration [17] is promising.

The low-lying surface vibrations certainly produce strong effects in the near- and sub-barrier fusion of  $^{40}\text{Ca} + ^{96}\text{Zr}$ , but, on top of that, couplings to  $Q > 0$  transfer channels bring further significant enhancements, even at the level of a few  $\mu\text{b}$ , where no indication of hindrance appears yet.

#### Acknowledgements

Thanks are due to V.V. Sargsyan for providing us with his calculations. We are very grateful to the XTU Tandem staff, to N. Toniolo for developing the new DAQ, and to M. Loriggiola for preparing targets of excellent quality. The research leading to these results has received funding from the European Union Seventh Framework Programme FP7/2007–2013 under Grant Agreement No. 262010-ENSAR. T.M. and S.S. were partially supported by the Croatian Ministry of Science, Education and Sports (Grant No. 0098-1191005-2890). H.E. is supported by the US Department of Energy, Office of Nuclear Physics, Contract No. DE-AC02-06CH11357.

#### References

- [1] M. Dasgupta, D.J. Hinde, N. Rowley, A.M. Stefanini, *Annu. Rev. Nucl. Part. Sci.* **48** (1998) 401.
- [2] C.L. Jiang, et al., *Phys. Rev. Lett.* **89** (2002) 052701.
- [3] M. Beckerman, et al., *Phys. Rev. C* **837** (25) (1982) 837; M. Beckerman, et al., *Phys. Rev. Lett.* **45** (1980) 1437.
- [4] R.A. Broglia, C.H. Dasso, S. Landowne, A. Winther, *Phys. Rev. C* **27** (1983) 2433; R.A. Broglia, C.H. Dasso, S. Landowne, G. Pollaro, *Phys. Lett. B* **133** (1983) 34.
- [5] J.J. Kolata, et al., *Phys. Rev. C* **85** (2012) 054603.
- [6] Z. Kohley, J.F. Liang, D. Shapira, C.J. Gross, R.L. Varner, J.M. Allmond, J.J. Kolata, P.E. Mueller, A. Roberts, *Phys. Rev. C* **87** (2013) 064612.
- [7] H. Timmers, et al., *Phys. Lett. B* **399** (1997) 35; H. Timmers, et al., *Nucl. Phys. A* **633** (1998) 421.
- [8] C.H. Dasso, S. Landowne, A. Winther, *Nucl. Phys. A* **407** (1983) 221.
- [9] V.I. Zagrebaev, *Phys. Rev. C* **67** (2003) 061601(R).
- [10] Ning Wang, Xizhen Wu, Zhuxia Li, *Phys. Rev. C* **67** (2003) 024604.
- [11] Huan-Qiao Zhang, Zu-Huan Liu, Feng Yang, Cheng-Jian Lin, Ming Ruan, Yue-Wei Wu, Zhu-Xia Li, Xi-Zhen Wu, Kai Zhao, Ning Wang, *Chin. Phys. Lett.* **22** (2005) 3048.
- [12] G. Pollaro, A. Winther, *Phys. Rev. C* **62** (2000) 054611.
- [13] G. Montagnoli, S. Beghini, F. Scarlassara, A.M. Stefanini, L. Corradi, C.J. Lin, G. Pollaro, A. Winther, *Eur. Phys. J. A* **15** (2002) 351.
- [14] A.M. Stefanini, et al., *Phys. Rev. C* **76** (2007) 014610.
- [15] A.M. Stefanini, et al., *Phys. Rev. C* **73** (2006) 034606.

- [16] F. Scarlassara, et al., *Prog. Theor. Phys. Suppl.* 154 (2004) 31.
- [17] V.V. Sargsyan, G.G. Adamian, N.V. Antonenko, W. Scheid, H.Q. Zhang, *Phys. Rev. C* 85 (2012) 024616.
- [18] V.V. Sargsyan, G.G. Adamian, N.V. Antonenko, W. Scheid, H.Q. Zhang, *Phys. Rev. C* 86 (2012) 034614.
- [19] V.V. Sargsyan, G. Scamps, G.G. Adamian, N.V. Antonenko, D. Lacroix, *Phys. Rev. C* 88 (2013) 064601.
- [20] G. Montagnoli, et al., *Phys. Rev. C* 85 (2012) 024607.
- [21] C.L. Jiang, et al., *Phys. Rev. C* 82 (2010) 041601(R).
- [22] G. Montagnoli, et al., *Phys. Rev. C* 87 (2013) 014611.
- [23] H.Q. Zhang, et al., *Phys. Rev. C* 82 (2010) 054609.
- [24] S. Kalkal, et al., *Phys. Rev. C* 81 (2010) 044610.
- [25] A.M. Stefanini, et al., *Eur. Phys. J. A* 49 (2013) 63.
- [26] W.S. Freeman, H. Ernst, D.F. Geesaman, W. Henning, T.J. Humanic, W. Kühn, G. Rosner, J.P. Schiffer, B. Zeidman, *Phys. Rev. Lett.* 50 (1983) 1563.
- [27] H. Esbensen, C.L. Jiang, K.E. Rehm, *Phys. Rev. C* 57 (1998) 2401.
- [28] C.L. Jiang, K.E. Rehm, H. Esbensen, D.J. Blumenthal, B. Crowell, J. Gehring, B. Glagola, J.P. Schiffer, A.H. Wuosmaa, *Phys. Rev. C* 57 (1998) 2393.
- [29] A.M. Stefanini, et al., *Phys. Rev. Lett.* 74 (1995) 864.
- [30] H. Esbensen, C.L. Jiang, A.M. Stefanini, *Phys. Rev. C* 82 (2010) 054621.
- [31] Ş. Mişicu, H. Esbensen, *Phys. Rev. C* 75 (2007) 034606.
- [32] H. Esbensen, Ş. Mişicu, *Phys. Rev. C* 76 (2007) 054609.
- [33] Ö. Akyüz, Å. Winther, in: R.A. Broglia, R.A. Ricci (Eds.), *Nuclear Structure and Heavy-Ion Physics, Course LXXVII, Varenna*, in: *Proc. Int. Sch. Phys. "Enrico Fermi"*, North Holland, Amsterdam, 1981.
- [34] A.M. Stefanini, et al., *Phys. Rev. C* 78 (2008) 044607.
- [35] A.M. Stefanini, et al., *Phys. Lett. B* 679 (2009) 95.
- [36] H. Esbensen, F. Videbaek, *Phys. Rev. C* 40 (1989) 126.
- [37] *Evaluated Nuclear Structure Data Files, National Nuclear Data Center, Brookhaven National Laboratory*, <http://www.nndc.bnl.gov/>.
- [38] T. Kibédi, R.H. Spear, *At. Data Nucl. Data Tables* 80 (2002) 35.
- [39] H. Esbensen, S. Landowne, *Nucl. Phys. A* 492 (1989) 473.
- [40] C.H. Dasso, A. Vitturi, *Phys. Lett.* 179 (1986) 337.
- [41] H. Esbensen, *Phys. Rev. C* 68 (2003) 034604.
- [42] H. Esbensen, C.L. Jiang, *Phys. Rev. C* 79 (2009) 064619.
- [43] C.L. Jiang, et al., *Phys. Lett. B* 640 (2006) 18.